Reviewer 3.

This manuscript studies the vertical structure and dynamics of the continental slope circulation in the South China Sea. Layer-integrated vorticity diagnostics from Primitive-Equation numerical simulations with idealized geometry are used to study the sensitivity of the circulation to the upper-layer inflow in the Luzon Strait. It is shown that the vertical structure of the circulation (respectively cyclonic, anticyclonic, and cyclonic for the top, middle and bottom layers) is linked to the surface intensified flow's interaction with the curved geometry of the marginal basin.

I see several major issues in the manuscript. Briefly, the most important ones involve the attribution of the middle and bottom layer's driving mechanisms, potentially significant spurious flows associated with pressure gradient errors in the simulations, and the quantification and interpretation of the viscous term in the model. Text and figures read generally fine, but there are English language problems in the text, and several figures lack axis labels. The major and minor points are detailed below.

Response: Thank you for the helpful suggestions and comments. In response to the reviewer's feedback, we have carefully examined the pressure gradient errors and improved the physical interpretation of the results. Additionally, we have refined the language throughout the manuscript and made enhancements to the figures. Below, we provide a detailed response to each comment.

Major points:

M1 (Section 2, pressure gradient errors): The known problem of spurious flow associated with numerical pressure gradient errors in terrain-following models such as ROMS always needs to be examined before a process study can be performed adequately. The authors need to show how the magnitude of the spurious circulation that arises in their model with an unforced, initially laterally-uniform stratification everywhere compares to the slope currents in their forced simulations. The physical signal of the slope currents is weak (less than 10 cm/s in the middle and bottom layers), and the spurious flow needs to be much smaller than that. With 30 vertical levels, a 5 km grid, and the O(1e-2) bottom slopes

involved, pressure gradient errors are likely to be non-negligible in the SCS's continental slope. Without smoothing the topography, the only solution is to refine the horizontal and vertical grids until the spurious flow becomes negligible. This numerical effect needs to be thoroughly examined before the results can be interpreted appropriately.

Response: Thanks for the reminder. In response to the reviewer's concerns, we examined the layered circulation and the magnitude of the bottom pressure gradient in an unforced scenario with an initially laterally uniform stratification (Figures R1 and R2). Overall, while some spurious flow associated with numerical pressure gradient errors was observed, no distinct circulation pattern was formed, and the magnitudes of these errors are significantly smaller than the mean circulation in the cases presented in the manuscript.

In this simulation, the strong upper-layer intrusion from the open ocean, combined with the contrasting mixing intensity that induces exchange currents, provides substantial external physical forcing. Additionally, the sigma layers were refined near the bottom layer to improve accuracy. Thus, we think the physical signal of the slope current, and the analysis are reliable.

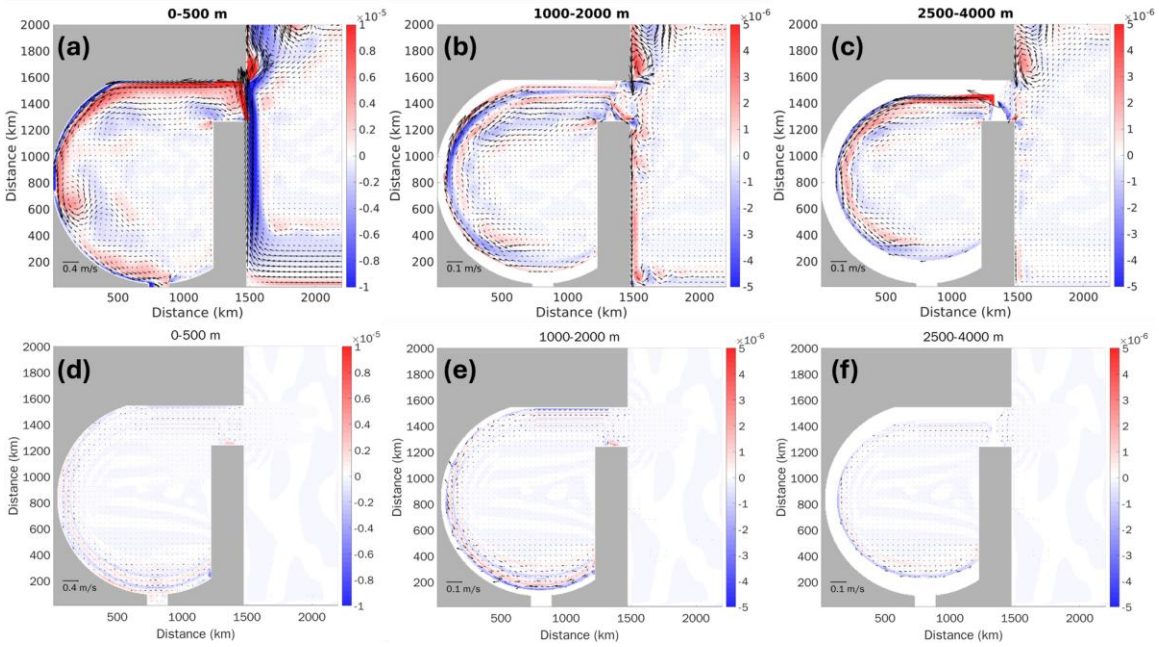

Figure R1. The horizontal circulation (arrows) and depth averaged vorticity (color) of (a) upper layer 0-500 m, (b) middle layer 1000-2000 m and (c) deep layer 2500-4000 m in the

standard case. The color indicates the depth-averaged vorticity in each layer. (e-f) are same as (a-c) but for the unforced simulation.

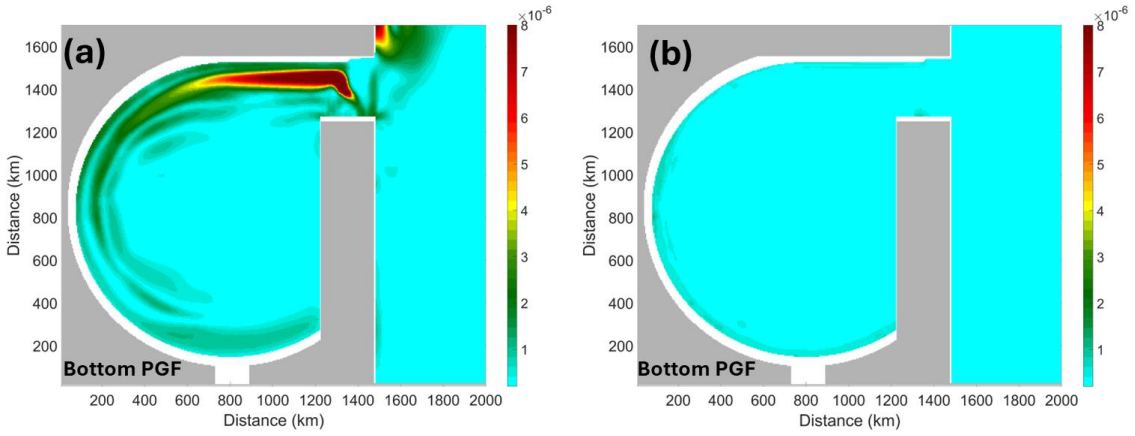

Figure R2. The magnitude of bottom pressure gradient force (PGF=$\sqrt{PGF_x^2 + PGF_y^2}$) in (a) standard case in manuscript and (b) unforced simulation.

M2: Related to point M1, what is the vertical spacing of the sigma levels? Are they refined near the surface and bottom to improve representation of the boundary layers?

Response: Yes, the sigma levels were refined near the surface and bottom (Figure R3). Near the surface and bottom, the vertical spacing is approximately 0.01 to improve the representation of the boundary layers.

In the revised manuscript, we clarified it:

Line 103-104: Near the surface and bottom boundaries, the vertical resolution is refined with spacing of approximately 0.01.

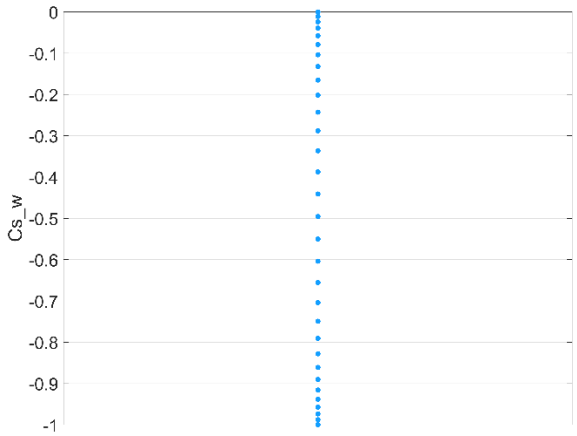

Figure R3. The vertical spacing of the sigma levels in the simulation.

M3: (lines 105-108): All results may be sensitive to these coefficient choices (particularly flow in the top and bottom layers). This needs to be thoroughly examined if a spatially-varying viscosity coefficient is used.

M4: Related to M3, what was the turbulent closure scheme used? This information is missing in the text.

Response: These two comments are related to the mixing coefficient in the simulation, so we addressed them together.

For the layered circulation in the middle and deep layers, they are mainly maintained by the outflux and deep intrusion through LS, respectively. According to previous investigations, exchange currents in the deep and middle layers are largely driven by density differences caused by contrasting turbulent mixing intensities (Tian et al., 2009; Yang et al., 2016; Zhu et al., 2019; Zhou et al., 2023). In the observation work of Yang et al (2016), they provided estimates of Kv for specific depth intervals: 500–1500 m, 1500 m to the bottom, and 500 m above the seafloor (Figure R4). Similarly, Wang et al. (2017) report Kv values of O(10^{-4} m^2 /s^2) in the continental shelf break region and O(10^{-3} m^2 /s^2) in deep waters.

In this study, we focused on exploring the response of the layered slope current, particularly in the semi-enclosed middle and deep layers, to changes in the upper-layer circulation.

Thus, in the simulation, we adopted the estimation in the observation of Yang et al (2017), without using a turbulent closure scheme. Similar approaches have been employed in our previous works and other studies (e.g., Cai et al., 2023; Emile-Geay and Madec, 2009; Huang and Jin, 2002; Quan and Xue, 2019; Zhao et al., 2020).

Although an idealized configuration was used, the results and processes observed in this simulation are generally consistent with established understandings from previous studies. The intensified turbulent mixing within the deep SCS basin gradually leads to a density difference between the two sides of the LS. Specifically, the deep SCS exhibits lower density compared to the Pacific basin (Figure R5). Under the density difference, the westward pressure gradient was formed that drives the deep intrusion from the open ocean towards the SCS. Associated with the simulated layered exchanging current, the layered circulations developed inside the SCS basin. The upper, middle, and deep layers exhibit circulation in cyclonic, anticyclonic, and cyclonic directions, respectively (Figure R5). Those features are consistent with established understandings from previous studies (e.g., Wang, Xie et al. 2011, Zhu et al., 2017, 2019; Cai, Chen et al. 2023; Zhou et al., 2023).

In the revised manuscript, we clarified those point:

Line 114-118: The K_v was designed based on observational work by Yang et al. (2016) and estimations by Wang et al. (2017) to form the circulation in the semi-enclosed middle and deep layers. Then, simulations were conducted to explore the response of the layered slope current, particularly in the semi-enclosed middle and deep layers, to changes in the upper-layer circulation

Line 142-151: Although the initial temperature and salinity distributions are horizontally uniform, the intensified turbulent mixing within the deep SCS basin gradually leads to a density difference between the two sides of the LS. Specifically, the deep SCS exhibits lower density compared to the Pacific basin (Figure S1). Under the density difference, the westward pressure gradient was formed that drives the deep intrusion from the open ocean towards the SCS. Those features are consistent with established understandings from previous studies (e.g., Wang, Xie et al. 2011, Zhu et al., 2017, 2019; Cai, Chen et al. 2023;

Zhou et al., 2023). Associated with the simulated layered exchanging current, the layered circulations developed inside the SCS basin. The upper, middle, and deep layers exhibit circulation in cyclonic, anticyclonic, and cyclonic directions, respectively (Figure S1).

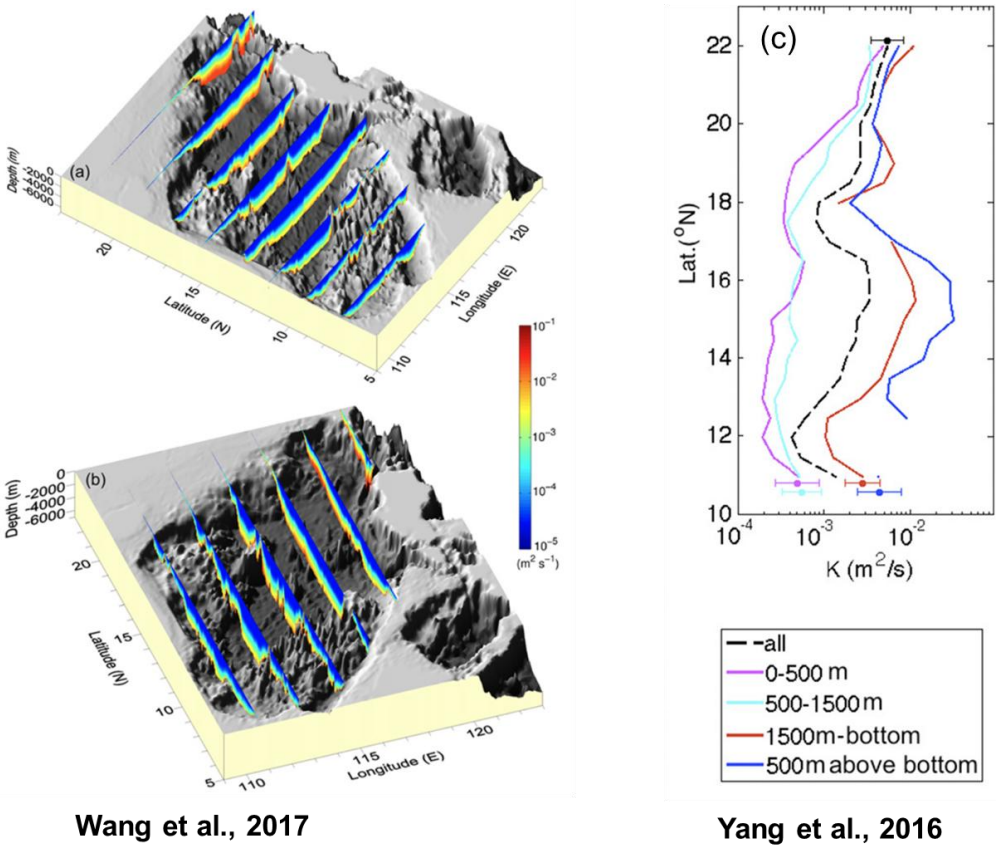

Figure R4. (a-b) The spatial distributions of the tide-induced diapycnal diffusivity estimated from internal tide energetics along the (a) zonal sections and (b) meridional sections. From Wang et al, 2017; (c) Depth-averaged diffusivity ($m^2\ s^{-1}$) for different layers in the meridional direction. The error bars indicate the uncertainty of standard deviation. From Yang et al., 2016

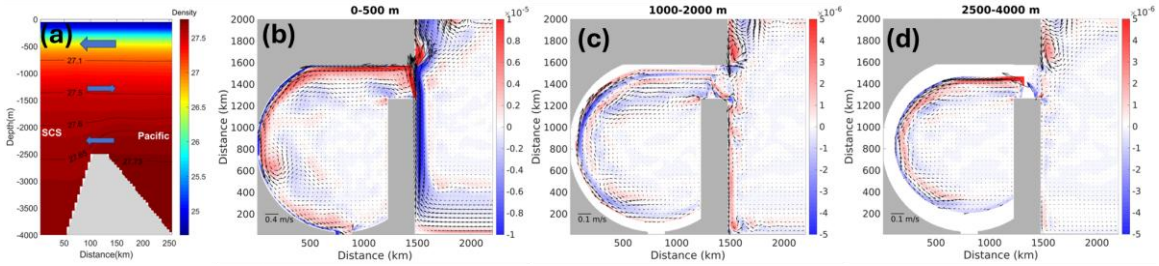

Figure R5. (a) Vertical transect of density (represented by color shading and contour lines) across the Luzon Strait. The left side represents the SCS basin, while the right side corresponds to the Pacific basin. Schematic arrows indicate the direction of the exchange flow between the two basins. (b-d) The horizontal circulation (arrows) and depth averaged vorticity (color) of (a) upper layer 0-500 m, (b) middle layer 1000-2000 m and (c) deep layer 2500-4000 m in the standard case.

Reference:

Cai, Z., D. Chen and J. Gan (2023). "Formation of the Layered Circulation in South China Sea With the Mixing Stimulated Exchanging Current Through Luzon Strait." Journal of Geophysical Research: Oceans 128(3).

Emile-Geay, J., and G. Madec, 2009: Geothermal heating, diapycnal mixing and the abyssal circulation. Ocean Sci., 5, 203-217, doi:10.5194/os-5-203-2009.

Huang, R. X., and X. Jin, 2002: Deep Circulation in the South Atlantic Induced by Bottom-Intensified Mixing over the Midocean Ridge. Journal of Physical Oceanography, 32, 1150-1164, doi:https://doi.org/10.1175/1520-0485(2002)032<1150:DCITSA>2.0.CO;2.

Quan, Q., and H. Xue, 2019: Influence of Abyssal Mixing on the Multilayer Circulation in the South China Sea. Journal of Physical Oceanography, 49, 3045-3060, doi:https://doi.org/10.1175/JPO-D-19-0020.1.

Yang, Q., W. Zhao, X. Liang, and J. Tian, 2016: Three-Dimensional Distribution of Turbulent Mixing in the South China Sea. J. Phys. Oceanogr., 46, 769–788, https://doi.org/10.1175/JPO-D-14-0220.1.

Wang, X., Z. Liu, and S. Peng, 2017: Impact of Tidal Mixing on Water Mass Transformation and Circulation in the South China Sea. J. Phys. Oceanogr., 47, 419–432, https://doi.org/10.1175/JPO-D-16-0171.1.

Wang, G., S.-P. Xie, T. Qu and R. X. Huang (2011). "Deep South China Sea circulation."

Geophysical Research Letters **38**(5): n/a-n/a.

Zhao, X., C. Zhou, X. Xu, R. Ye, and W. Zhao, 2020: Deep circulation in the South China Sea simulated in a regional model. Ocean Dynamics, 70, 1461-1473, doi:10.1007/s10236-020-01411-2.

Zhu, Y., J. Sun, Y. Wang, Z. Wei, D. Yang and T. Qu (2017). "Effect of potential vorticity flux on the circulation in the South China Sea." Journal of Geophysical Research: Oceans **122**(8): 6454-6469.

Zhu, Y., Sun, J., Wang, Y., Li, S., Xu, T., Wei, Z. and Qu, T., 2019. Overview of the multi-layer circulation in the South China Sea. *Progress in Oceanography*, *175*, pp.171-182.

Zhou, C., Xiao, X., Zhao, W. et al. Increasing deep-water overflow from the Pacific into the South China Sea revealed by mooring observations. Nat Commun 14, 2013 (2023). https://doi.org/10.1038/s41467-023-37767-4

M5 (lines 113-114): Is the system at a near-steady state at this point? Some metric such as a global KE time series should show this clearly and help determine how long the simulations need to be. Also, I assume this is a 5-year average? If so, please mention that here.

Response: Thank you for the reminder from the reviewer. In response to the reviewer's concern, we've checked the time series of the basin-averaged vorticity in different layers (Figure R6). Generally, even for the middle and deep layers, the simulation time is sufficient to reach the steady state.

Yes, the 5-year average was used.

In the revised manuscript, we clarify this point:

Line 126-127: The simulation ran for 25 years, with the analysis was conducted on the results from the final 5 years average after the layered circulation reached a stable state.

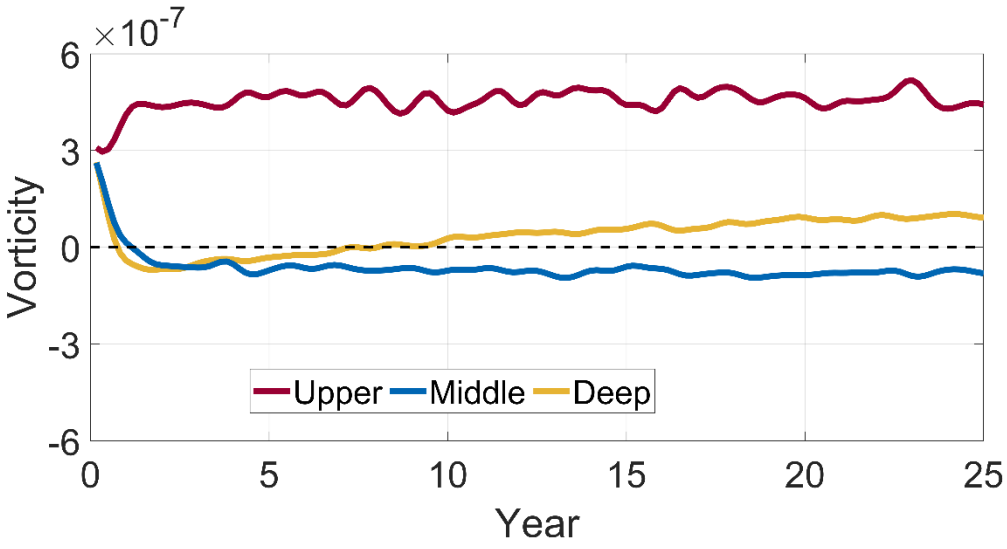

Figure R6. Time series of the domain-averaged vorticity averaged in the upper 500 m (Upper), 1000-2000 m (Middle), and below 2500 m (Deep)

M6 (Figure 2, Section 2): The topography in the southern boundary of the LS has a more irregular shape than the SCS and Pacific parts of the domain. What is the reason for this choice, and how sensitive are the results to this geometry (compared to a configuration where the LS's southern boundary joins the interior of the SCS smoothly like what is seen in the LS's northern boundary in Figure 2a)?

Response: In this study, our aim is to understand how changes in the upper-layer circulation modulate the layered circulation over the meandering slope, particularly in the semi-enclosed middle and deep layers. To facilitate the formation of the upper-layer cyclonic circulation, a shallow opening with a depth of approximately 400 m was configured to allow outflux, enabling the upper-layer intrusion from the Luzon Strait. This opening represents the relatively shallow straits in the southern part of SCS. It was not specifically designed but simply provided to allow the outflux.

Considering that the primary regions of coupling among the three layers are not near the southern boundary, and the depth of the southern opening is relatively shallow, its influence on the overall results is minimal.

In the revised manuscript, we clarified this point:

Line 106-107: The SCS was opened to the south with the depth of 400 m (Figure 2a), to allow the upper-layer intrusion to develop intrinsically during the simulation.

M7 (Lines 176-177, Equation 1): There is no separation between the vertical and horizontal viscosity terms. It is therefore impossible to distinguish physical bottom Ekman pumping from numerical lateral viscosity.

M8 (lines 190-192, 216-217): I think it is indeed likely that the near-bottom cross-slope flow dominates near-bottom vertical velocity, but this has not been shown directly. Besides near-bottom flow across isobaths, bottom Ekman pumping can also produce important vertical velocity and vortex stretching. This effect is not examined here because the term is excluded from the analysis and from Equation 2 (the approximately equal sign is an assumption rather than a result). Figure 5c shows that bottom friction may be important in the bottom layer's vorticity budget, though it is unclear because the viscous term combines lateral and vertical friction.

Response: These two comments are related to the viscous term and effect of the bottom Ekman pumping, so we addressed them together.

Due to the magnitude of the horizontal viscosity term is much smaller than the vertical one (Figure R7), it was combined with the vertical term, and we did not separate the two terms. In the revised manuscript, we clarified that this point to avoid misunderstanding:

Line 197-198: The horizontal viscosity is much smaller than vertical viscosity term and they are included in the $\overrightarrow{VIS}$ term for simplicity.

For the Equation (2), following reviewer's suggestion, we examined the effect of the Ekman pumping by modifying it as:

$$-\nabla_h \cdot \int_{-H}^{z} \vec{\bar{V}}_h dz \approx$$

$$-\nabla_h \cdot \int_{-H}^{z} \vec{\bar{V}}_{h\_geo} dz - \nabla_h \cdot \int_{-H}^{z} \vec{\bar{V}}_{h\_vis} dz = \overbrace{-(\bar{v}_{b\_geo} H_y + \bar{u}_{b\_geo} H_x)}^{CGT_b} + \underbrace{\frac{\beta}{f} \int_{-H}^{z} \bar{v}_{geo} dz}_{\beta\ effect} \overbrace{-\nabla_h \cdot \int_{-H}^{z} \vec{\bar{V}}_{h\_vis} dz}^{Fric} \quad (2)$$

One more term was added $-\nabla_h \cdot \int_{-H}^{z} \vec{\bar{V}}_{h\_vis} dz$ (Fric), which represent the effect of the bottom Ekman pumping that induced by the bottom stress of the slope current.

As pointed out by the reviewer, the deep layer (Figure R7 and Figure 5c in the manuscript) has quite large vertical viscosity terms. We examined its effect on the deep ζ_DIV (ζ_DIV_D), which features a downward flux (negative value) over the northern slope and upward flux (positive value) over the southern part. Generally, the $Fric$ has contribution to the deep ζ_DIV_D and features with a relatively uniform downward motion. It has the same direction as the Ekman transport induced by the bottom stress of the deep cyclonic slope current. However, the primary pattern and magnitude of the ζ_DIV_D are determined by the bottom geostrophic cross-isobath transport (CGT_b) (Figure R8).

Additionally, bottom Ekman pumping is induced by bottom frictional stress, which responds to and is only affected by the bottom layer circulation, while the bottom pressure is modulated by the motions of water in the entire water column above it. In this study, we observed that changes in the upper-layer circulation intensify the middle and deep circulations over the slope. The changes in the upper layer circulation may not affect the bottom friction directly but modulate the bottom pressure distribution over the slope. This modulation then leads to the stronger vertical stretching/squeezing within the water column, and in turn impacts the circulation. Thus, in the analysis, we pay more attention to the effect of bottom cross-isobath geostrophic transport.

Following reviewer's concerns, in the revised manuscript, the updated Equation (2) and Figure R8 was adopted, and we mentioned the role of the bottom Ekman pumping.

Line 265-273: For the deep layer, the viscosity term has an important effect in the vorticity budget (Figure 5c). Similarly, the $Fric_D$ term contributes to the deep ζ_DIV_D and is characterized by a relatively uniform downward motion (Figure 7d). However, the primary pattern and magnitude of the ζ_DIV_D are largely controlled by the CGT_b that the pressure distribution maintained the mean downwelling in the northern side and the upwelling over the southern slope (Figure 7b, d). Since the $Fric_D$ is induced by the bottom frictional stress as response to the deep layer slope current, while the bottom pressure is modulated by the

motions of water in the entire water column above it, we further examine the maintenance of the bottom pressure over the slope

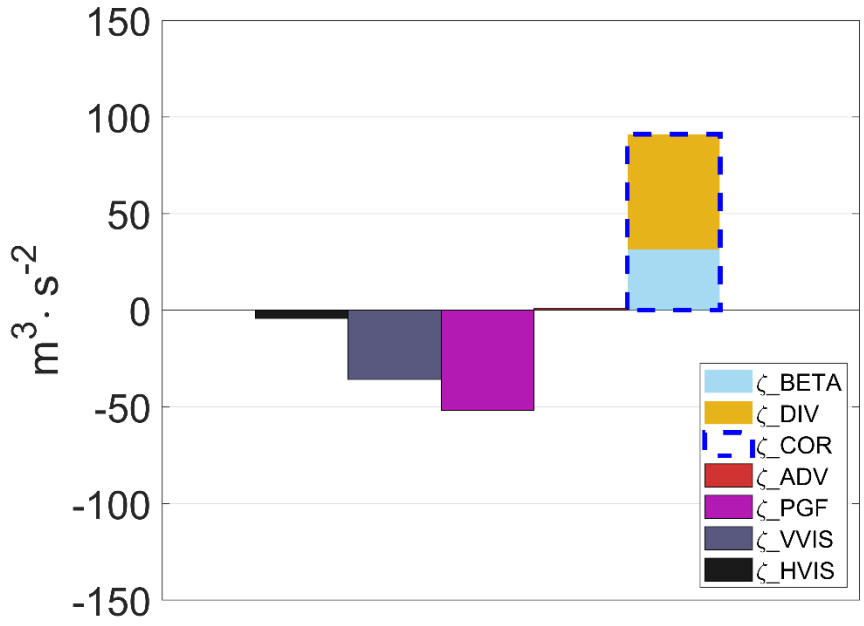

Figure R7. Similar as Figure 5c in the manuscript. The layered-integrated vorticity budget (Equation 1) for the standard case in the layers of 2,500–4,000 m. The ζ_VIS is decomposed into the horizontal (ζ_HVIS) and vertical (ζ_VVIS) component, respectively.

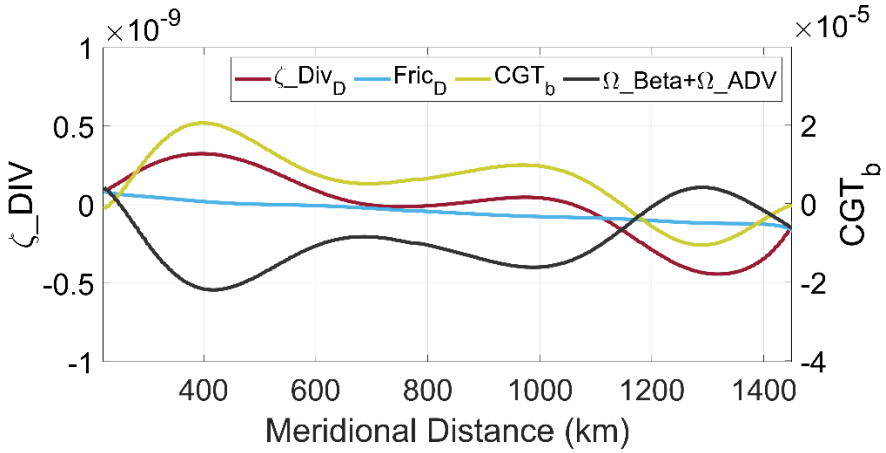

Figure R8. Meridional changes of the ζ_DIV_D, $Fric_D$, CGT_b and $\Omega\_BETA + \Omega\_ADV$ over the slope. This figure will be used as Figure 7d in the revised manuscript.

M9 (lines 238-240): Source/sink Stommel and Arons-like dynamics does not include topography, so it cannot be consistent with a flow where cross-slope bottom geostrophic flow is dominating the bottom layer dynamics. The only way to test this type of dynamics unambiguously is to perform experiments with a vertical wall (as in the adjacent rectangular basin representing the Pacific) instead of a slope.

Response: Thanks for the reminder from reviewer. Following reviewer's comment, we removed this sentence to avoid misunderstanding.

M10: Since the model has a 5 km resolution, it should be eddy-resolving in the SCS, where the first baroclinic deformation radius is around 60 km in the SCS (e.g., Figure 6 in Chelton et al, 1998 or Figure 8 in LaCasce & Groeskamp, 2020). Because mesoscale eddies and sloping topography are present, a competing theory for the cyclonic layers' flow in a basin like this is eddy-slope interaction (Neptune Effect, e.g., Holloway, 1987, see also Stewart et al., 2024 and references therein). It may be possible to test this hypothesis by changing the horizontal resolution: If by coarsening the grid spacing until eddies are no longer resolved results do not change, then an eddy-free interpretation may be correct. But if the Neptune effect is important in one or both cyclonic layers, these layers will have stronger flow with finer, eddy-resolving resolutions, and the interpretation needs to be revisited.

M11: What is the first baroclinic deformation radius in the model (especially in the SCS's deep basin, and in the SCS's slope)? This information is relevant for addressing point M10 and for comparing how well the model represents the real SCS's stratification.

Response: These two comments are related to the formation dynamics of layered circulation in the SCS, thus we addressed them together.

As a semi-enclosed marginal sea, the circulation in the SCS is closely related to the external flux through the LS. Generally, the cyclonic-anticyclonic-cyclonic circulation in the upper, middle, and deep layers is maintained by the influx-outflux-influx pattern through the LS (Figure R9). The theoretical understanding was obtained based on the potential vorticity

conservation constraint (Yang and Price, 2000; Zhu et al, 2007) or depth-integrated vorticity dynamics (Equation 1 and Figure 5 in the manuscript). In the depth-integrated vorticity dynamics, the net planetary vorticity influx/outflux maintained the cyclonic/anticyclonic circulations in each layer and is mainly balanced by the bottom pressure torque and the bottom friction curl. These insights have provided robust physical explanations for layered circulation in various regions (e.g., Karcher et al., 2007; Zhu et al., 2017; Kastner et al., 2024; Jiang et al., 2024; Li and Gan et, 2023).

When numerical simulations reduce resolution, it may not adequately resolve the slope. As an alternative approach, flat-bottom simulations could be conducted to check the formation of basin circulation without eddy-slope interaction (Figure R10). With flat bottom, the external flux could drive the basin scale circulation, and the direction of this circulation aligns well with predictions from potential vorticity conservation constraint or depth-integrated vorticity dynamics.

In this study, we focused on basin-scale circulation, and those theoretical frameworks effectively explain the processes of basin circulation and the coupling among different layers. Following these frameworks, we examined the mechanisms by which changes in upper-layer circulation modulate layered circulation. We appreciate the reviewer's suggestion to explore the Neptune Effect in future investigations. In the revised manuscript, we have highlighted that the Neptune Effect could be another potential mechanism influencing layered circulation in marginal seas like the SCS. We plan to explore this in our future studies.

Line 355-359: In addition to the processes revealed in this study, other mechanisms, such as the Neptune Effect involving the eddy-slope interaction (e.g., Holloway, 1987, Stewart et al., 2024), may also play a role in influencing circulation dynamics in marginal seas like the SCS. It will be incorporated into our future investigations to improve understanding.

For the deformation radius, following reviewer concern, we calculated the deformation radius using the method of Chelton et al. (1998) (Figure R11). Over the deep basin, the deformation radius is approximately 70 km, consistent with the values reported by Chelton

et al. (1998) and LaCasce & Groeskamp (2020). Over the slope, the deformation radius gradually decreases to approximately 35 km as the depth decreases.

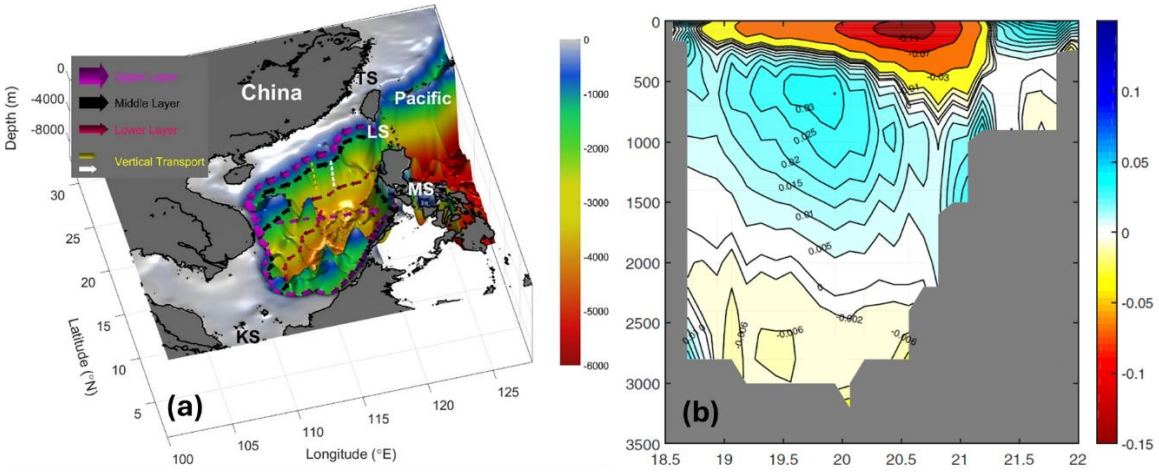

Figure R9. (a) Schematic annual mean CAC circulation in the South China Sea. Color contours represent bathymetry (m). LS: Luzon Strait; TS: Taiwan Strait; MS: Mindoro Strait; and KS: Karimata Strait. (From Cai et al., 2020). (b) zonal geostrophic velocity in the Luzon Strait at 120845'E. Positive values indicate eastward flow in m/s. The dashed lines represent the interfaces of density layers in the Luzon Strait. (From Zhu et al., 2017)

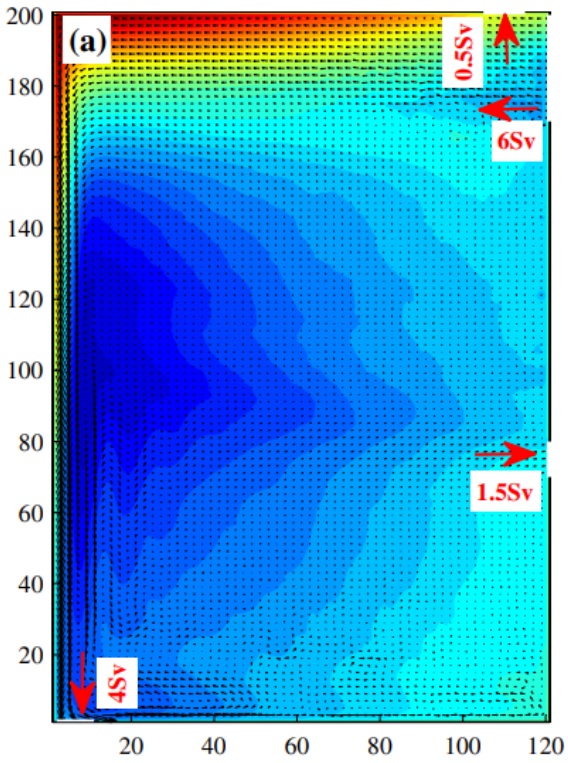

Figure R10. Basin circulation with flat bottom driven by the external flux (From Chen and Xue, 2014)

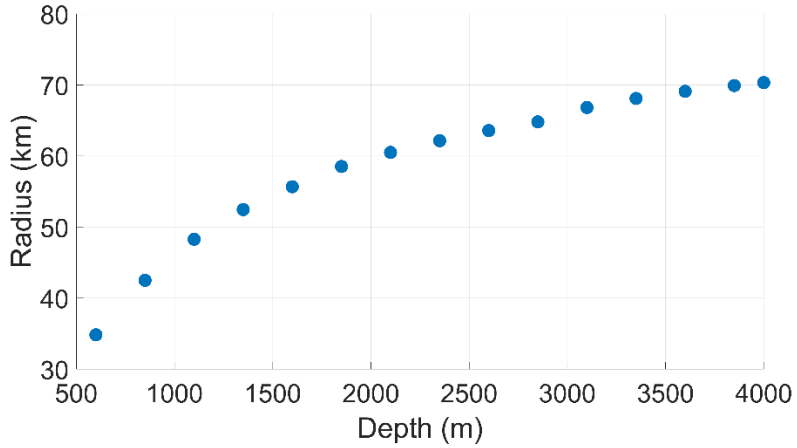

Figure R11. Changes of the first baroclinic deformation radius with the depth over the slope at the latitude of 15.5 N.

Reference:

Cai, Z., Gan, J., Liu, Z., Hui, C. R., & Li, J. (2020). Progress on the formation dynamics of the layered circulation in the South China Sea. *Progress in Oceanography*, *181*, 102246.

Chen, G., & Xue, H. (2014). Westward intensification in marginal seas. *Ocean Dynamics*, *64*, 337-345.

Karcher, M., F. Kauker, R. Gerdes, E. Hunke, and J. Zhang (2007), On the dynamics of Atlantic Water circulation in the Arctic Ocean, *J. Geophys. Res.*, 112, C04S02, doi:10.1029/2006JC003630.

Kastner, S. E., G. Pawlak, S. N. Giddings, A. E. Adelson, R. Collin, and K. A. Davis, 2024: The Influence of Caribbean Current Eddies on Coastal Circulation in the Southwest Caribbean Sea. *J. Phys. Oceanogr.*, **54**, 2119–2132, https://doi.org/10.1175/JPO-D-24-0049.1.

Li, J., & Gan, J. (2023). How the forcing dynamics of the western boundary currents in the Pacific respond to the North Equatorial Current. Progress *in Oceanography*, *210*, 102950.

Jiang, H., Xin, X., Xu, H. *et al.* Three-layer circulation in the world deepest hadal trench. *Nat* Commun 15, 8949 (2024). https://doi.org/10.1038/s41467-024-53370-7

Yang, J., Price, J., 2000. Water-mass formation and potential vorticity balance in an abyssal ocean circulation. J. Mar. Res. 58 (5), 789–808. https://doi.org/10.1357/ 002224000321358918.

Zhu, Y., J. Sun, Y. Wang, Z. Wei, D. Yang and T. Qu (2017). "Effect of potential vorticity flux on the circulation in the South China Sea." Journal of Geophysical Research: Oceans 122(8): 6454-6469.

M12 (lines 322-323, Data Availability statement): The repository in the DOI (https://doi.org/10.5281/zenodo.13835538) contains only *.mat files. Based on the file names, I assume these can be used to replot the figures, but they are not sufficient to reproduce the results. To ensure reproducibility, the authors need to provide all the source codes used in the calculations, as well as the configuration files for the ROMS model applications.

Response: We appreciate reviewer's suggestion on the data availability. The .mat files there are the averaged results from the last five years of the model output. For the source codes and configurations, these can be made available upon request to the corresponding author. We revised the Data availability accordingly to ensure clarity, thanks!

Minor points:

m1: (lines 30, 232, 311): The term "Cascading" is typically used to refer to a specific process driven by surface buoyancy loss. To avoid ambiguity, I suggest using "downwelling" instead.

Response: Thanks for the kind suggestions, we corrected it as downwelling in the revised manuscript.

m2 (lines 94-95): Is the southern model strait the same depth as the model Luzon Strait?

Response: The southern strait is quite shallow with a depth of ~400 m. We clarify it in the revised manuscript.

Line 106-107: The SCS was opened to the south with the depth of 400 m (Figure 2a), to allow the upper-layer intrusion to develop intrinsically during the simulation

m3: Figure 1: The real topographic gradients in the SCS are more difficult to see with these color limits. It may be better to change the lower limit to something closer to 4 km, even though this would saturate the color scale in the Western Pacific troughs.

Response: Thank you for your suggestion regarding the colormap in Figure 1. We understand that adjusting the lower limit to approximately 4 km could enhance the visibility of topographic gradients in the South China Sea (SCS). However, such a change would result in the saturation of the color scale in other regions

Given that we have included transects to illustrate the slope, we prefer to maintain the original colormap. Thanks.

m4 (line 292): Stimulated or simulated?

Response: Thanks for your careful review. We have corrected it to "simulated" in the revised manuscript.

m5 (line 303): "curved" is probably a better description, Since the basin is circular.

Response: Thanks for kind suggestion, we corrected it as curved in the revised manuscript.

m6 (Figures 6, 7 and others): Several axes are missing labels, units, or both.

Response: We correct those figures, thanks so much!

m7 (Figure 6d): It may be better to flip Figure 6d 90 degrees clockwise to have depth in the y-axis.

Response: Thank you for the kind suggestion. We intentionally used the horizontal axis to represent depth, so that the transition from left to right corresponds to moving from shallow to deep regions, being similar as the horizontal map.

References:

Chelton et al. (1998): Geographical Variability of the First Baroclinic Rossby Radius of Deformation, Journal of Physical Oceanography.

LaCasce & Groeskamp (2020): Baroclinic Modes over Rough Bathymetry and the Surface Deformation Radius, Journal of Physical Oceanography.

Holloway (1987): Systematic forcing of large-scale geophysical flows by eddy-topography interaction, Journal of Fluid Mechanics.

Stewart et al. (2024): Formation of eastern boundary undercurrents via mesoscale eddy rectification, Journal of Physical Oceanography.